Inorg. Chem. **2006**, *45*, 1326–1337

A Comparative Mechanistic Study of the Reversible Binding of NO to a Water-Soluble Octa-Cationic Fe^{III} Porphyrin Complex

Joo-Eun Jee,[†] Maria Wolak,[†] Domenico Balbinot,[§] Norbert Jux,*[,§] Achim Zahl,[†] and Rudi van Eldik*[,†]

Institute for Inorganic Chemistry, University of Erlangen-Nürnberg, Egerlandstrasse 1, 91058 Erlangen, Germany, Institute for Organic Chemistry, University of Erlangen-Nürnberg, Henkestrasse 42, 91054 Erlangen, Germany

Received August 5, 2005

The water-soluble, non-μ-oxo dimer-forming porphyrin, [5,10,15,20-tetrakis-4′-*t*-butylphenyl-2′,6′-bis-(*N*-methylene-(4″-*t*-butylpyridinium))porphyrinato]iron(III) octabromide, $(P^{8+})Fe^{III}$, with eight positively charged substituents in the ortho positions of the phenyl rings, was characterized by UV–vis and ^1H NMR spectroscopy and ^{17}O NMR water-exchange studies in aqueous solution. Spectrophotometric titrations of $(P^{8+})Fe^{III}$ indicated a pK_{a1} value of 5.0 for coordinated water in $(P^{8+})Fe^{III}(H_2O)_2$. The monohydroxo-ligated $(P^{8+})Fe^{III}(OH)(H_2O)$ formed at $5 < pH < 12$ has a weakly bound water molecule that undergoes an exchange reaction, $k_{ex} = 2.4 \times 10^6\ s^{-1}$, significantly faster than water exchange on $(P^{8+})Fe^{III}(H_2O)_2$, viz. $k_{ex} = 5.5 \times 10^4\ s^{-1}$ at 25 °C. The porphyrin complex reacts with nitric oxide to yield the nitrosyl adduct, $(P^{8+})Fe^{II}(NO^+)(L)$ ($L = H_2O$ or OH^-). The diaqua-ligated $(P^{8+})Fe^{III}(H_2O)_2$ binds and releases NO according to a dissociatively activated mechanism, analogous to that reported earlier for other $(P)Fe^{III}(H_2O)_2$ complexes. Coordination of NO to $(P^{8+})Fe^{III}(OH)(H_2O)$ at high pH follows an associative mode, as evidenced by negative $\Delta S^{\ddagger}_{on}$ and $\Delta V^{\ddagger}_{on}$ values measured for this reaction. The observed ca. 10-fold decrease in the NO binding rate on going from six-coordinate $(P^{8+})Fe^{III}(H_2O)_2$ ($k_{on} = 15.1 \times 10^3\ M^{-1}\ s^{-1}$) to $(P^{8+})Fe^{III}(OH)(H_2O)$ ($k_{on} = 1.56 \times 10^3\ M^{-1}\ s^{-1}$ at 25 °C) is ascribed to the different nature of the rate-limiting step for NO binding at low and high pH, respectively. The results are compared with data reported for other water-soluble iron(III) porphyrins with positively and negatively charged meso substituents. Influence of the porphyrin periphery on the dynamics of reversible NO binding to these $(P)Fe^{III}$ complexes as a function of pH is discussed on the basis of available experimental data.

Introduction

Interactions of nitric oxide, an important biological messenger synthesized in vivo by NO synthase, with heme-containing proteins form the basis of many physiological and pathophysiological processes mediated by NO. Due to the fact that NO is reactive toward both iron(III) and iron(II) hemes, nature used a variety of structural and electronic features to tune the affinity of (P)Fe porphyrin centers for NO, such that its physiological roles can be effected while at the same time its potential pathophysiological actions are prevented. In addition to the oxidation state of iron, a number of other factors associated with the immediate heme surrounding (such as number and identity of axial iron ligands, type of heme substituents, etc.) influence the rate of NO binding and release as well as the stability and chemical properties of the resulting heme nitrosyls.[1] To elucidate the role of these different factors, numerous spectroscopic, structural, and mechanistic studies focus on the interactions of NO with heme centers in hemoproteins and its synthetic models.[1]

Our own contribution in this area involves in-depth mechanistic studies on interactions of nitric oxide with ferriheme proteins[2] and synthetic iron(III) porphyrin models.[3,4] These investigations are aimed at understanding the influence of the porphyrin microenvironment in a given (P)-

* To whom correspondence should be addressed. E-mail: vaneldik@chemie.uni-erlangen.de (R.v.E.), jux@organik.uni-erlangen.de (N.J.).
[†] Institute for Inorganic Chemistry.
[§] Institute for Organic Chemistry.

(1) (a) Ford, P. C.; Lorkovic, I. M. *Chem. Rev.* **2002**, *102*, 993 and references therein. (b) Ford, P. C.; Laverman, L. E.; Lorkovic, I. M. *Adv. Inorg. Chem.* **2003**, *54*, 2003 and references therein. (c) Scheidt, W. R.; Ellison, M. K. *Acc. Chem. Res.* **1999**, *32*, 350 and references therein. (d) Wyllie, G. R. A.; Scheidt, W. R. *Chem. Rev.* **2002**, *102*, 1067 and references therein.

10.1021/ic051339v CCC: $33.50
Published on Web 12/24/2005

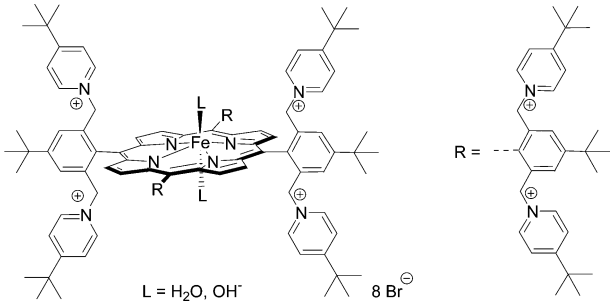

Figure 1. Structure of $(P^{8+})Fe^{III}(L)_2$.

Fe^{III} system on the rate and mechanism of NO binding and release and on the stability of the resulting $(P)Fe^{II}(NO^+)$ species (i.e., $\{FeNO\}^6$ nitrosyls according to the Enemark and Feltham notation[1]) toward subsequent reactions in solution. In this context, we have recently undertaken systematic studies on the influence of the porphyrin ligand (modified in size, overall charge, and electron-donating ability by introducing various meso phenyl substituents) on the properties and reactivity of the iron center for water-soluble ferric porphyrins.[3−5] As a continuation of our earlier work in this field, we report here on the speciation of a highly positively charged water-soluble iron(III) porphyrin (P^{8+})-Fe^{III} (Figure 1) in aqueous medium and present the results of mechanistic studies on its reactivity toward NO. In the latter context, variable pH, temperature, and pressure-dependent stopped-flow measurements provided a detailed kinetic and mechanistic description of the reversible binding of NO to $(P^{8+})Fe(H_2O)_2$ and $(P^{8+})Fe(OH)(H_2O)$ present in aqueous solution at low and high pH, respectively. The results are compared with water-exchange data for these complexes and with kinetic data reported for other water-soluble porphyrins. A feasible interpretation of the reactivity patterns observed within the series of complexes studied is presented on the basis of these data. The biological significance of our results is highlighted.

Experimental Section

Materials. The water-soluble $(P^{8+})Fe^{III}$ (**1**) was synthesized and characterized as described before.[6] [5,10,15,20-Tetrakis(4-*N*-methylpyridyl)porphinato]iron(III) (**2**), $[(4\text{-TMPyP})Fe^{III}(H_2O)(OH)](Tos)_4$, was purchased from Frontier Scientific Ltd. Fine Chemicals, Utah, USA. NO gas (Messer Griesheim or Riessner Gase, ≥99.5 vol %) was cleaned from trace amounts of higher nitrogen oxides by passing it through a concentrated KOH solution and an Ascarite II column (NaOH on silica gel, Sigma-Aldrich). All other chemicals used in this study were of analytical reagent grade. Tris, Bis-Tris, and $ClCH_2COOH$, used for the preparation of buffer solutions, were purchased from Sigma-Aldrich.

Solution Preparation. Solutions were prepared from deionized water and handled in gastight glassware under oxygen-free conditions due to the oxygen sensitivity of NO and (P)Fe(NO) nitrosyls. Oxygen-free nitrogen was used to deoxygenate the solutions. Tris, Bis-Tris, and $ClCH_2COOH/ClCH_2COO^-$ buffers (0.05 M) were used to prepare solutions of desired pH, which was adjusted by the addition of HNO_3 or KOH. Due to the relative pressure sensitivity of the pH of the $ClCH_2COOH/ClCH_2COO^-$ buffer system, the high-pressure stopped-flow measurements at pH 2 were performed in the absence of a buffer, and the solution acidity was adjusted with HNO_3. The ionic strength of the solutions (0.1 M) was kept constant by the addition of KNO_3.

Measurements. pH measurements were performed on a Methrom 623 pH meter. UV−vis spectra were recorded in gastight cuvettes on a Shimadzu UV-2100 spectrophotometer equipped with a thermostated (±0.1 °C) cell compartment. ^1H NMR spectra of iron porphyrin solutions in D_2O (10 mM) were measured on a Bruker Avance DPX300NM spectrometer. The desired pD was adjusted with DCl and NaOD, and TMSP (trimethylsilyl propionate) was used as a reference.

Kinetics Measurements. Stopped-Flow Studies. Stopped-flow kinetic measurements at ambient pressure were performed on an SX 18.MV (Applied Photophysics) stopped-flow apparatus. In a typical experiment, a deoxygenated buffer solution was mixed in varying volume ratios with a saturated NO solution in a gastight syringe to obtain the appropriate NO concentration (0.2−1.8 mM). The NO solution was then rapidly mixed with deoxygenated iron(III) porphyrin in a 1:1 volume ratio in a stopped-flow apparatus. Kinetics of the reaction of **1** with NO were monitored at 395 and 430 nm at pH 2 and 8, respectively. All kinetic experiments were performed under pseudo-first-order conditions, i.e., with at least 10-fold excess of nitric oxide over $(P^{8+})Fe^{III}$. The rates of NO binding and release (k_{on} and k_{off}) were determined from the slopes and intercepts of linear plots of k_{obs} versus [NO], respectively, as described in Results and Discussion. Rate constants reported are mean values of at least five kinetic runs, and the quoted uncertainties are based on standard deviation. To confirm the kinetic data for the release of NO obtained from the intercepts of plots of k_{obs} vs [NO], an alternative NO-trapping method was used to measure the rate of NO dissociation from $(P^{8+})Fe^{II}(NO^+)$ directly at pH 8. This was done by rapid mixing of a $(P^{8+})Fe^{II}(NO^+)$ solution containing a small excess of NO with aqueous solutions of $[Ru^{III}(edta)(H_2O)]^-$ (1 mM) (an efficient NO scavenger[7]) to give $[Ru^{III}(edta)NO]^-$ and free $(P^{8+})Fe^{III}$, as evidenced by the observed UV−vis spectral changes. The kinetics of NO release were followed in a stopped-flow spectrophotometer at 432 nm. The first-order rate constants determined in this way were in good agreement with those determined from the intercepts of the plots of k_{obs} versus [NO] for the formation of $(P^{8+})Fe^{II}(NO^+)$. High-pressure stopped-flow experiments were performed at pressures up to 130 MPa on a custom-built instrument, described previously.[8] Kinetic traces were analyzed with the use of the OLIS KINET (Bogart, GA, 1989) set of programs.

The kinetics of reversible NO binding to $(4\text{-TMPyP})Fe^{III}(OH)$ (**2-OH**) was studied at pH 7.6 (0.07 M Tris), ionic strength 0.09 M (adjusted with $NaNO_3$), and an iron porphyrin concentration of 6×10^{-6} M. The UV−vis spectra of the iron porphyrin solutions

(2) (a) Laverman, L. E.; Wanat, A.; Oszajca, J.; Stochel, G.; Ford, P. C.; van Eldik, R. *J. Am. Chem. Soc.* **2001**, *123*, 285. (b) Franke, A.; Stochel, G.; Jung, Ch.; van Eldik, R. *J. Am. Chem. Soc.* **2004**, *126*, 4181.
(3) (a) Theodoridis, A.; van Eldik, R. *J. Mol. Catal. A: Chem.* **2004**, *224*, 197. (b) Franke, A.; Stochel, G.; Suzuki, N.; Higuchi, T.; Okuzono, K.; van Eldik, R. *J. Am. Chem. Soc.* **2005**, *127*, 5360.
(4) (a) Wolak, M.; van Eldik, R. *J. Am. Chem. Soc.* **2005**, *127*, 13312. (b) Jee, J.-E.; Eigler, S.; Hampel, F.; Jux, N.; Wolak, M.; Zahl, A.; Stochel, G.; van Eldik, R. *Inorg. Chem.* **2005**, *44*, 7717.
(5) Schneppensieper, T.; Zahl, A.; van Eldik, R. *Angew. Chem., Int. Ed.* **2001,** *40*, 1678.
(6) Guldi, D. M.; Rahman, G. M. A.; Jux, N.; Balbinot, D.; Hartnagel, U.; Tagmatarchis, N.; Prato, M. *J. Am. Chem. Soc.* **2005**, *127*, 9830.
(7) Wanat, A.; Schneppensieper, T.; Karocki, A.; Stochel, G.; van Eldik, R. *J. Chem. Soc., Dalton Trans.* **2002**, 941.
(8) Spitzer, M.; Gartig, F.; van Eldik, R. *Rev. Sci. Instrum.* **1988**, *59*, 2092.

recorded prior to the kinetic measurements were identical with that reported for the (4-TMPyP)Fe(OH) monomer.[9] The absence of bands, characteristic for the μ-oxo dimer[9] of **2**, confirms that the monomeric monohydroxo form is the reactive species under the selected experimental conditions. The reaction with NO was followed at 433 nm. Stopped-flow studies at ambient and elevated pressures were performed in an analogous way as described for **1**.

^{17}O NMR Water-Exchange Measurements. Rate constants for water exchange on the paramagnetic $(P^{8+})Fe^{III}$ complex and the corresponding activation parameters, $\Delta H^{\ddagger}_{ex}$, $\Delta S^{\ddagger}_{ex}$, and $\Delta V^{\ddagger}_{ex}$, were measured at pH = 2.0 and 8.0 by ^{17}O NMR line-broadening technique. Aqueous solutions of $(P^{8+})Fe^{III}$ (20 mM) were prepared at pH 2.0 (adjusted with HNO_3) and pH 8 (0.05 M Tris buffer). Both solutions were 0.1 M in KNO_3 for an approximate adjustment of the ionic strength. To each solution was added 10% of the total sample volume of enriched ^{17}O-labeled water (normalized 19.2% $^{17}O\ H_2O$, D-Chem Ltd). A sample containing the same components, except for $(P^{8+})Fe^{III}$, was used as a reference. Variable-temperature and -pressure FT ^{17}O NMR spectra were recorded at a frequency of 54.24 MHz on a Bruker Advance DRX 400WB spectrometer. The temperature dependence of ^{17}O line broadening was studied in the range 278−353 K. A homemade high-pressure probe[10] was used for the variable-pressure experiments performed at the selected temperature (313 K at pH 2 and 298 K at pH 8) and in the pressure range 1−150 MPa. The sample was placed in a standard 5-mm NMR tube cut to a length of 45 mm. Hydrostatic pressure was transmitted to the sample by a movable macor piston, and the temperature was controlled as described elsewhere.[10] The reduced transverse relaxation times ($1/T_{2r}$) were calculated for each temperature and pressure from the difference in the line widths observed in the presence and absence of the metal complex ($\Delta\nu_{obs} - \Delta\nu_{solvent}$). The reduced transverse relaxation time is related to the exchange rate constant $k_{ex} = 1/\tau_m$ (where τ_m is the mean coordinated solvent lifetime) and to the NMR parameters by the Swift and Connick equation,[11,12]

$$\frac{1}{T_{2r}} = \pi \frac{1}{P_m}(\Delta\nu_{obs} - \Delta\nu_{solvent}) = \frac{1}{\tau_m}\left\{\frac{T_{2m}^{-2} + (T_{2m}\tau_m)^{-1} + \Delta\omega_m^2}{(T_{2m}^{-1} + \tau_m^{-1})^2 + \Delta\omega_m^2}\right\} + \frac{1}{T_{2os}} \quad (1a)$$

where P_m is the mole fraction of water coordinated to the Fe^{III} ion, T_{2os} represents the outer-sphere contribution to T_{2r} arising from long-range interactions of unpaired electrons of Fe^{III} with the water outside of the coordination sphere, T_{2m} is the transverse relaxation time of water in the inner coordination sphere in the absence of chemical exchange, and $\Delta\omega_m$ is the difference in the resonance frequency of ^{17}O nuclei in the first coordination sphere of the metal and in the bulk solvent. In the present system, the contributions of $1/T_{2m}$ and $1/T_{2os}$ to $1/T_{2r}$ are negligible, so that eq 1a can be reduced to

$$\frac{1}{T_{2r}} = \pi \frac{1}{P_m}(\Delta\nu_{obs} - \Delta\nu_{solvent}) = \frac{1}{\tau_m}\left\{\frac{\Delta\omega_m^2}{\tau_m^{-2} + \Delta\omega_m^2}\right\} \quad (1b)$$

Taking into account that the temperature dependence of k_{ex} is given by eq 1c (taken from transition state theory), the NMR and kinetic parameters were calculated by the use of a nonlinear least-squares method applied to eq 1b in which $1/\tau_m$ was replaced by eq 1c.

$$k_{ex} = \frac{1}{\tau_m} = (k_B T/h)\exp\{(-\Delta V^{\ddagger}_{ex}/RT)P\} \quad (1c)$$

The temperature dependence of $\Delta\omega_m$ was assumed to be a simple reciprocal function A/T,[11] where A was determined as a parameter in the treatment of the line-broadening data. The exchange rate constant is assumed to have a simple pressure dependence given by

$$k_{ex} = 1/\tau_m = k_{ex}^{\ 0}\exp\{(-\Delta V^{\ddagger}_{ex}/RT)P\} \quad (1d)$$

where $k_{ex}^{\ 0}$ is the rate constant for solvent exchange at atmospheric pressure. The pressure-dependent measurements were performed at a temperature close to the optimal exchange region (i.e., around the maximum of the plot of $\ln(1/T_{2r})$ versus $1/T$). The reduced relaxation time T_{2r} and the value of $\Delta\omega_m$ (calculated using the value of A, determined from the temperature dependence and assumed to be pressure independent[11d]) were substituted into eq 1b to determine k_{ex} at each pressure. The resulting plot of $\ln(k_{ex})$ versus pressure was linear, and the volume of activation was calculated directly from the slope ($-\Delta V^{\ddagger}_{ex}/RT$). The values of $k_{ex}^{\ 0}$ obtained from the plot of $\ln(k_{ex})$ versus P by extrapolation to atmospheric pressure was in good agreement with the corresponding value for $k_{ex}^{\ 0}$ from the temperature-dependent measurements at ambient pressure.

Results and Discussion

Spectroscopic Data for the Speciation of $(P^{8+})Fe^{III}$. The speciation of **1** in an aqueous medium of different pHs was studied by UV−vis, ^{1}H NMR, and ^{17}O NMR techniques. Spectrophotometric titration of a $(P^{8+})Fe^{III}$ solution in the pH range 1−10 resulted in the spectral changes presented in Figure 2a. As can be seen from these data, an increase in pH from 3 to 7 leads to a gradual shift of the peaks at 402 nm ($\epsilon = 8.6 \times 10^4\ M^{-1}\ cm^{-1}$) and 529 nm ($\epsilon = 7.4 \times 10^3\ M^{-1}\ cm^{-1}$) to 416 nm ($\epsilon = 9.2 \times 10^4\ M^{-1}\ cm^{-1}$) and 595 nm ($\epsilon = 7.2 \times 10^3\ M^{-1}\ cm^{-1}$), respectively. This is accompanied by the formation of a band at 340 nm. The observed pattern of spectral changes is analogous to that reported for other water-soluble iron(III) porphyrins for the formation of monohydroxo-ligated species from the corresponding diaqua-ligated $(P)Fe(H_2O)_2$.[9,13−16] The $pK_{a1} = 5.05 \pm 0.07$, determined from a plot of absorbance at 390 and 460 nm versus pH (inset in Figure 2a), is thus ascribed to equilibrium 2 (the presence of water in the deprotonated form of **1-H$_2$O** is inferred from NMR data reported below).

$$(P^{8+})Fe(H_2O)_2 \rightleftarrows (P^{8+})Fe(OH)(H_2O) + H^+ \qquad pK_{a1} = 5.0 \quad (2)$$

As can be seen from the data in Table 1, the pK_{a1} determined for **1-H$_2$O** lies in the lower range of pK_{a1} values reported

(9) Tondreau, G. A.; Wilkins, R. G. *Inorg. Chem.* **1986**, *25*, 2745.
(10) Zahl, A.; Neubrand, A.; Aygen, S.; van Eldik, R. *Rev. Sci. Instrum.* **1994,** *65*, 882.
(11) (a) Swift, T. J.; Connick, R. E. *J. Chem. Phys.* **1962**, *37*, 307. (b) Swift, T. J.; Connick, R. E. *J. Chem.* Phys. **1964**, *41*, 2553. (c) Newman, K. E.; Meyer, F. K.; Merbach, A. E. *J. Am. Chem. Soc.* **1979**, *101*, 1470.
(12) Schneppensieper, T.; Seibig, S.; Zahl, A.; Tregloan, P.; van Eldik, R. *Inorg. Chem.* **2001**, *40*, 3670.
(13) Zipplies, M. F.; Lee, W. A.; Bruice, T. C. *J. Am. Chem. Soc.* **1986**, *108*, 4433.
(14) (a) Kobayashi, N. *Inorg. Chem.* **1985**, *24*, 3324. (b) Kobayashi, N.; Koshiyama, M.; Osa, T.; Kuwana, T. *Inorg. Chem.* **1983**, *22*, 3608.

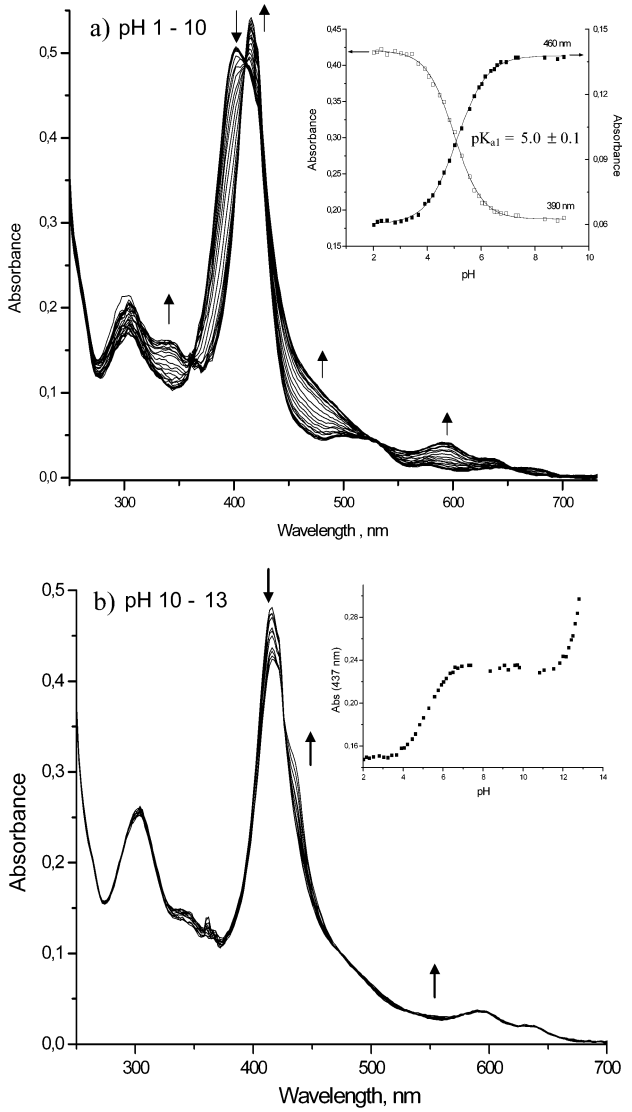

Figure 2. (a) Changes in the UV−vis spectrum of (P^{8+})Fe^{III} (**1**) in the pH range 1−10. (Inset) Fit of the plots of Abs$_{(390)}$ and Abs$_{(460)}$ versus pH to a sigmoidal function. (b) UV−vis spectral changes for **1** in the pH range 10−13. (Inset) Evolution of absorbance at 437 nm in the whole studied pH range. Experimental conditions: [**1**] = 1.2×10^{-5} M, I = 0.1 M (KNO_3), T = 25 °C.

for water-soluble iron(III) porphyrins, thus reflecting the increased positive charge on the iron(III) center in (P^{8+})-Fe^{III}(H$_2$O)$_2$.

On further increasing the pH, an onset of spectral changes featuring a second pH-dependent equilibrium is observed, as shown in Figure 2b. A pattern of UV−vis spectral changes similar to these in Figure 2b was previously reported for the formation of (TMPyP)Fe^{III}(OH)$_2$ complexes from the corresponding monohydroxo-ligated species, for which pK_{a2} values of 10.9, 12.2, and 12.3 (for 2-TMPyP, 3-TMPyP, and 4-TMPyP porphyrins, respectively) were measured.[14] It is therefore assumed that (P^{8+})Fe(OH)(H$_2$O) (denoted as **1-OH** in the remainder of text) deprotonates to (P^{8+})Fe(OH)$_2$ at pH > 12. However, because this process is of minor importance for the topic of this report, further speciation studies concentrated on the nature of porphyrin forms occurring in the pH range 1−11.

Table 1. pK_{a1} Values and β-Pyrrole ^{1}H NMR Chemical Shifts of Synthetic Water-Soluble Iron(III) Porphyrins

Iron(III) porphyrin [a]	*meso* phenyl substituent	pK_{a1} [b]	β-pyrrole ^{1}H (ppm) [c]	
			(P)Fe(H$_2$O)$_2$	(P)Fe(OH)
(P^{8+})Fe [d]	(P^{8+})	5.0 [d]	66	83
(4-TMPyP^{4+})Fe	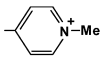	5.5	70 [e]	NA [e]
(3-TMPyP^{4+})Fe		5.9	NA	NA
(2-TMPyP^{4+})Fe		5.1	73 [f]	84 [f]
(TF$_4$TMAP^{4+})Fe		6.0	72 [g]	85 [g]
(TPPS^{4-})Fe	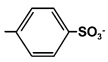	7.0	52 [e]	NA [e]
(DMPS^{4-})Fe [h]	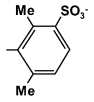	7.2	45	80
(TMPS^{4-})Fe [i]	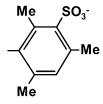	6.9	43	82
(P^{8-})Fe [j]	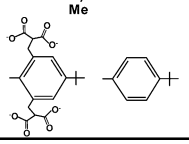	9.3	45.6; 46.7	82

[a] The quoted charge represents the overall charge of the meso substituents in a given porphyrin ligand. [b] Values taken from: Gruhn, N. E.; Lichtenberger, D. L.; Ogura, H.; Walker, F. A. *Inorg. Chem.* 1999, *38*, 4023, unless otherwise stated. [c] Referenced to TMPS. [d] This work. [e] Reference 22. [f] Reference 21. [g] Reference 24b. [h] Reference 13. [i] Reference 4a. [j] Reference 4b.

In this respect, **1-H$_2$O** and **1-OH** were studied by ^{1}H and ^{17}O NMR spectroscopy. The ^{1}H NMR spectra of (P^{8+})Fe^{III} recorded at pD 2 and 8 (Figure S1) indicated that the β-pyrrole ^{1}H signal (which serves as a sensitive probe for the spin and ligation state of iron(III) porphyrins)[17,18] appears at 66 ppm at pD 2 and moves to ca. 83 ppm at high pH. The chemical shift of the β-pyrrole resonance ($\delta_{\beta-py}$) observed at a low pH is close to that reported for other positively charged (P)Fe(H$_2$O)$_2$ complexes (Table 1) and evidences the presence of six-coordinate (P^{8+})Fe(H$_2$O)$_2$ species in which the Fe(III) center is weakly spin-admixed (ca. 10% contribution of the intermediate $S = {}^3/_2$ spin state to the predominant $S = {}^5/_2$ spin state can be estimated for this complex on the

(15) Miskelly, G. M.; Webley, W. S.; Clark, Ch. R.; Buckingham, D. A. *Inorg. Chem.* **1988**, *27*, 3773.
(16) El-Awady, A. A.; Wilkins, P. C.; Wilkins, R. G. *Inorg. Chem.* **1985**, *24*, 2053.
(17) Walker, F. A. Proton and NMR Spectroscopy of Paramagnetic Metalloporphyrins. In *The Porphyrin Handbook*; Kadish, K. M., Smith, K. M., Guilard, R., Eds.; Academic Press: New York, 1999; Vol. 5.
(18) Ikezaki, A.; Nakamura, M. *Inorg. Chem.* **2002**, *41*, 6225 and references therein.

Table 2. Rate Constants (at 298 K) and Activation Parameters for Water-Exchange Reactions on Water-Soluble Iron(III) Porphyrins

		(P)Fe(H_2O)$_2$				(P)Fe(OH)			
	iron(III) porphyrin	$k_{ex}/10^5$ s^{-1}	$\Delta H^{\ddagger}_{ex}$ kJ/mol	$\Delta S^{\ddagger}_{ex}$ J/mol·K	$\Delta V^{\ddagger}_{ex}$ cm^3/mol	$k_{ex}/10^5$ s^{-1}	$\Delta H^{\ddagger}_{ex}$ kJ/mol	$\Delta S^{\ddagger}_{ex}$ J/mol·K	$\Delta V^{\ddagger}_{ex}$ cm^3/mol
1	$(P^{8+})Fe^a$	0.55 ± 0.01	53 ± 3	$+28 \pm 9$	$+1.5 \pm 0.2$	24 ± 6	32.5 ± 0.4	-14 ± 1	$+1.1 \pm 0.2$
2	$(TMPyP^{4+})Fe^b$	4.5 ± 0.1	71 ± 2	$+100 \pm 6$	$+7.4 \pm 0.4$	*c*			
3	$(TPPS^{4-})Fe^b$	20 ± 1	67 ± 2	$+99 \pm 10$	$+7.9 \pm 0.2$	*c*			
4	$(P^{8-})Fe^d$	77 ± 1	61 ± 6	$+91 \pm 23$	$+7.4 \pm 04$	*e*			
5	$(TMPS^{4-})Fe^f$	210 ± 10	61 ± 1	$+100 \pm 5$	$+11.9 \pm 0.3$	*g*			

[a] This work. [b] Reference 5. [c] Formation of μ-oxo dimers at porphyrin concentrations required for NMR measurements precludes reliable studies on water exchange. [d] Reference 4b. [e] No water-exchange process was detected for non-dimerizing **4-OH**, compare ref 4b. [f] Reference 4a. [g] The effect of **5-OH** on the bulk water line width observed in variable temperature ^{17}O NMR studies, although detectable, was too small to allow its quantitative analysis and determination of k_{ex} and the corresponding activation parameters for the water-exchange reaction, compare ref 4a.

basis of $\delta_{\beta-py}$[18]). The broad β-pyrrole resonance at 83 ppm observed at a high pH is diagnostic for a monomeric high-spin monohydroxo-ligated iron(III) porphyrin.[19−22] The lack of resonances at ca. 13 ppm (i.e., in the spectral region where β-pyrrole resonances of $(Fe^{III}(P))_2O$ dimers are typically observed[19,22]) excludes the formation of dimeric μ-oxo-bridged species at high pH.

Figure 3 shows the results of relaxation-time measurements for ^{17}O NMR nuclei of bulk water in solutions of **1** at pH 2 and 8. It is evident from these data that water exchange at the Fe(III) center occurs in both diaqua- and monohydroxo-ligated forms of **1**. Detailed variable temperature and pressure measurements allowed for the determination of rate constants (k_{ex}) and activation parameters ($\Delta H^{\ddagger}_{ex}$, $\Delta S^{\ddagger}_{ex}$, and $\Delta V^{\ddagger}_{ex}$) for this process, as summarized in Table 2. For comparison reasons, Table 2 also reviews the corresponding values reported for other water-soluble iron(III) porphyrins studied to date.[4,5] As can be seen from these data, the k_{ex} determined for **1-H_2O** (viz. 5.5×10^4 s^{-1}) is the smallest of the values reported for (P)Fe(H_2O)$_2$ porphyrins. Thus, the lability of the metal center in **1-H_2O** is decreased by the influence of the positively charged meso substituents on the porphyrin periphery, which apparently stabilize the $Fe^{III}-H_2O$ bond (presumably mainly through inductive electronic effects). The positive signs of $\Delta S^{\ddagger}_{ex}$ and $\Delta V^{\ddagger}_{ex}$ suggest a dissociatively activated mode for the water-exchange process in **1-H_2O**, as also found for the other six-coordinate $(P)Fe^{III}(H_2O)_2$ species. However, the absolute values of these activation parameters are much smaller than those observed for the other diaqua-ligated ferric porphyrins. Clearly, the degree of bond breaking in the transition state changes from very substantial in negatively charged **5-H_2O** to almost negligible in the highly positively charged **1-H_2O**, for which the water-exchange mechanism can be described as pure interchange (**I**).

The data presented in Figure 3b indicate a rapid water-exchange reaction at the Fe(III) center of the monohydroxo-ligated form **1-OH.** The k_{ex} value determined for this process (2.4×10^6 s^{-1} at 298 K) is ca. 50-fold larger as compared to that measured for **1-H_2O** at a low pH. The slightly negative activation entropy and small positive activation volume (viz. $\Delta S^{\ddagger}_{ex} = -14 \pm 1$ J mol^{-1} K^{-1}, $\Delta V^{\ddagger}_{ex} = +1.1 \pm 0.2$ cm^3 mol^{-1}) are indicative of an interchange mechanism in which the degree of bond breakage and bond formation in the transition state are comparable. The observed acceleration of water exchange on **1-OH** as compared to **1-H_2O** is in agreement with the expected *trans*-labilizing effect of the OH^- ligand on the dynamics of simple substitution processes such as water-exchange reactions.[23]

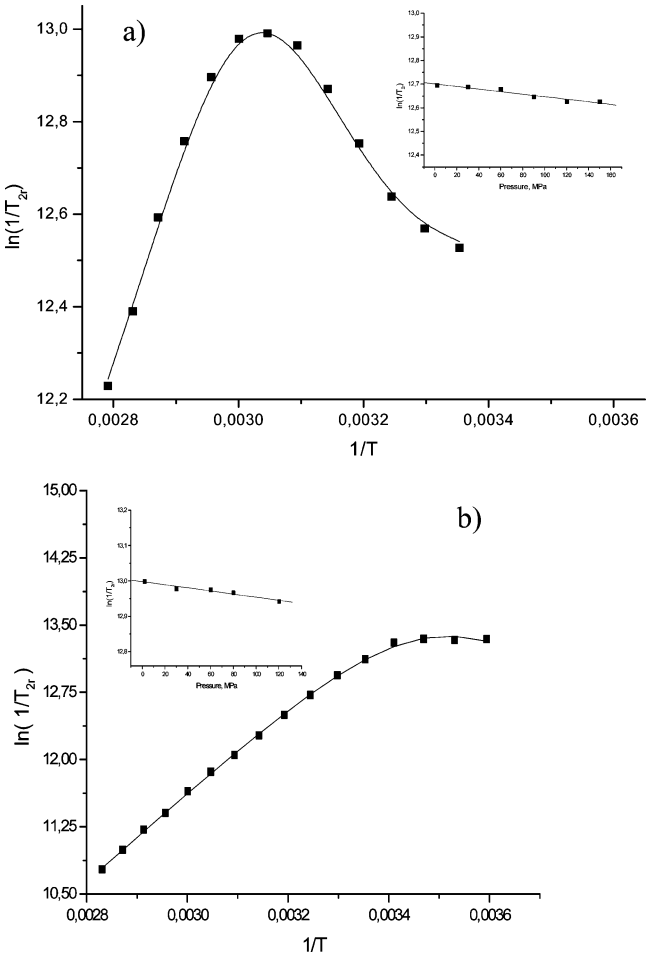

Figure 3. (a) Plot of $\ln(1/T_{2r})$ versus $1/T$ for water exchange on **1-H_2O** at ambient pressure. Fit of experimental data to eq 1 allows determination of $A = (2.1 \pm 0.1) \times 10^8$ and k_{ex}, $\Delta H^{\ddagger}_{ex}$, and $\Delta S^{\ddagger}_{ex}$ as reported in Table 2. (Inset) Plot of $\ln(1/T_{2r})$ versus pressure measured at 313 K. (b) Plot of $\ln(1/T_{2r})$ versus $1/T$ for water exchange on **1**-OH at ambient pressure. Fit of experimental data to eq 1 yields $A = (3.67 \pm 0.04) \times 10^8$ and k_{ex}, $\Delta H^{\ddagger}_{ex}$, and $\Delta S^{\ddagger}_{ex}$, as reported in Table 2. (Inset) Plot of $\ln(1/T_{2r})$ versus pressure measured at 298 K.

(19) Cheng, R.-J.; Grażyński, L.; Balch, A. *Inorg. Chem.* **1982**, *21*, 2412.
(20) Woon, T. C.; Shirazi, A.; Bruice, T. *Inorg. Chem.* **1986**, *25*, 3845.
(21) Reed, R. A.; Rodgers, K. R.; Kushmeider, K.; Spiro, T. *Inorg. Chem.* **1990**, *29*, 2883.
(22) Ivanca, M. A.; Lappin, A. G.; Scheidt, W. R. *Inorg. Chem.* **1991**, *30*, 711 and references therein.

As indicated by earlier literature reports, the high-spin monohydroxo-ligated iron(III) porphyrins may exist in solution as five-coordinate (P)Fe(OH)[19,20,24] or six-coordinate (P)-Fe(OH)(Solv) species.[24] Although the formation of (P)Fe-(OH) is promoted in noncoordinating solvents,[19,20] dynamic equilibria between the five- and six-coordinate (P)Fe(OH) and (P)Fe(OH)(H_2O) forms, respectively, were observed in water-containing solutions (eq 3), with the latter form being the main porphyrin species at high water contents.[24]

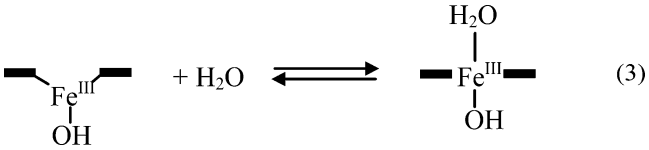

(3)

Relevant literature data[24] and the results of our ^{17}O NMR water-exchange studies performed for the monohydroxo-ligated forms of **1**, **4**, and **5** (Table 2) suggest that the tendency of (P)Fe^{III}(OH) to bind the sixth (H_2O) ligand, although evidently smaller than that exhibited by (P)Fe-(H_2O),[24] can be modulated by the nature of the porphyrin ring substituents. Thus, although no water exchange could be observed by ^{17}O NMR measurements for highly negatively charged (P^{8-})Fe(OH) (**4**) (suggesting that **4-OH** exists predominantly in the five-coordinate form), small (but clearly detectable) line-broadening effects observed for **5-OH** point to the presence of a fraction of (TMPS)Fe(OH)(H_2O) in equilibrium with the prevailing five-coordinate (TMPS)Fe-(OH) form. In the case of **1-OH**, the exchange of bulk and coordinated water at the iron(III) center is clearly evident from the line-broadening data. This shows that the affinity of the iron(III) center in (P^{8+})Fe(OH) for the axial H_2O ligand is increased by the highly positively charged porphyrin periphery, such that (P^{8+})Fe(OH)(H_2O) is the main (or exclusive) porphyrin form present in solution at pH > pK_{a1}. Such a conclusion is in line with UV−vis data indicating deprotonation of the aqua ligand in (P^{8+})Fe(OH)(H_2O) at pH > 12.

In principle, two possible structures can be envisaged for **1-OH** in aqueous solution, as depicted below.[19,20,24,25]

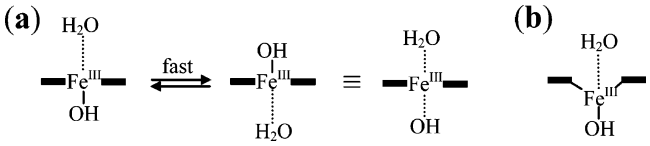

Although the exact coordination geometry cannot be unequivocally assigned on the basis of our experimental results, structure (a) is assumed to be more probable on the basis of structural data reported for other high-spin six-coordinate iron(III) porphyrins[26] and, thus, will be used throughout this work to depict the mono-hydroxo species **1-OH**.

(23) Cusanelli, A.; Frey, U.; Ritchens, D. T.; Merbach, A. E. *J. Am. Chem. Soc.* **1996**, *118*, 5265 and references therein.
(24) (a) La, T.; Miskelly, G. M.; Bau, R. *Inorg. Chem.* **1997**, *36*, 5321. (b) La, T.; Miskelly, G. M. *J. Am. Chem.* Soc. **1995**, *117*, 3613.
(25) Evans, D. R.; Reed, Ch. A. *J. Am. Chem. Soc.* **2000**, *122*, 4660 and references therein.
(26) Scheidt, W. R.; Reed, Ch. A. *Chem. Rev.* **1981**, *81*, 543.

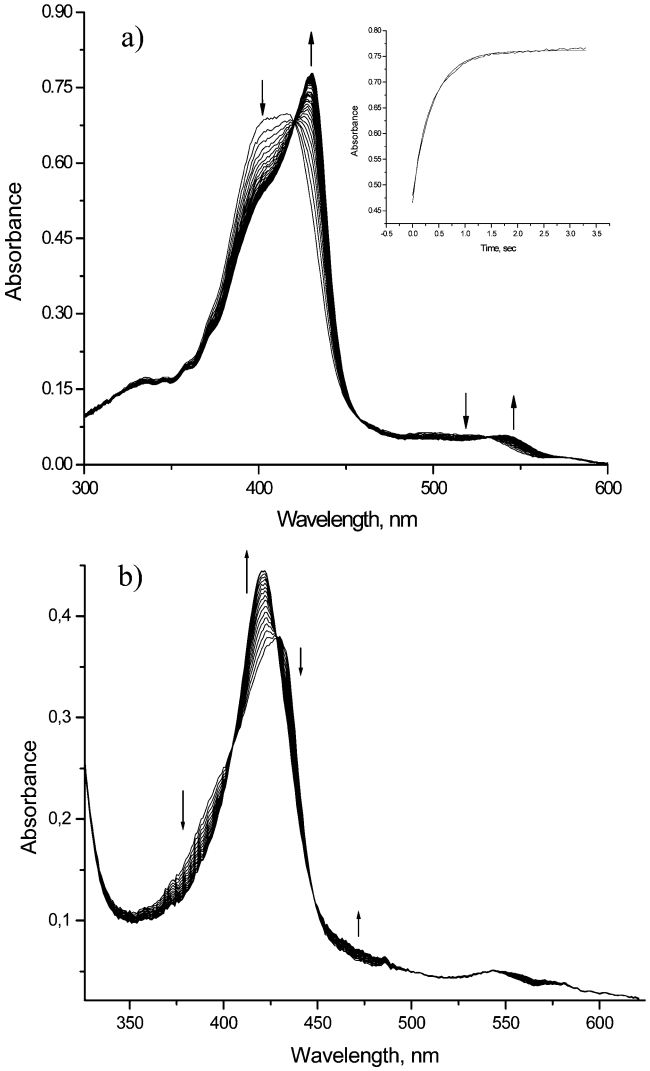

Figure 4. (a) Spectral changes accompanying rapid binding of NO (1×10^{-3} M) to **1-H_2O** (2×10^{-5} M) at pH 2 ($T = 5$ °C). (Inset) Fit of a kinetic trace recorded at 432 nm to a single-exponential function. (b) Subsequent slow (minute time scale) spectral changes for the conversion of the (P^{8+})Fe^{II}(NO^+) nitrosyl complex into the final product (P^{8+})Fe^{II}-(NO) via reductive nitrosylation.

All in all, the spectroscopic studies described above indicate the presence of six-coordinate (P^{8+})Fe(H_2O)$_2$ at pH < 5, in which the Fe−H_2O bond is strengthened by the electron-withdrawing influence of the porphyrin meso substituents. The six-coordinate (P^{8+})Fe(OH)(H_2O) (**1-OH**) is assumed to be the predominant (or sole) form of **1** in the pH range 6−12. The additional acid−base equilibrium observed for **1** at pH > 12 is ascribed to the formation of a dihydroxo-ligated complex, (P^{8+})Fe(OH)$_2$.

Reversible Binding of NO to (P^{8+})Fe^{III}(H_2O)$_2$. The addition of NO gas to a deoxygenated solution of **1-H_2O** at pH 2 leads to a rapid spectral change that involves a shift of the Soret and Q-bands from 402 and 526 nm to 430 and 542 nm, respectively, as reported in Figure 4a. The initially formed (P^{8+})Fe^{II}(NO^+) product (representing an {FeNO}^{6} nitrosyl) is not stable but undergoes further reductive nitrosylation[27] to form (P^{8+})Fe^{II}(NO) (an {FeNO}^{7} nitrosyl) on a time scale of several minutes. The final spectrum with Soret and Q-bands at 420 and 552 nm (Figure 4b),

Table 3. Rates and Activation Parameters for the Reversible Binding of NO to **1-H$_2$O** and **1-OH**

$(P^{8+})Fe(H_2O)_2$				$(P^{8+})Fe(OH)(H_2O)$				
T °C	P MPa	$k_{on}/10^3$ $M^{-1}\,s^{-1}$	k_{off} s^{-1}	T °C	P MPa	$k_{on}/10^3$ $M^{-1}\,s^{-1}$	k_{off} s^{-1}	k_{off}[a] s^{-1}
5		1.6 ± 0.1	2.3 ± 0.1	5		0.43 ± 0.02	0.71 ± 0.01	0.6 ± 0.1
10		2.8 ± 0.1	3.7 ± 0.1	10		0.61 ± 0.06	1.20 ± 0.03	1.0 ± 0.1
15		5.3 ± 0.2	8.5 ± 0.2	15		0.84 ± 0.03	2.04 ± 0.02	1.8 ± 0.1
20		10.5 ± 0.2	14.9 ± 0.2	20		1.12 ± 0.05	3.52 ± 0.03	2.9 ± 0.1
25		15.1 ± 0.9	26.3 ± 0.5	25		1.56 ± 0.06	6.22 ± 0.03	4.8 ± 0.1
5.5	10	1.14 ± 0.01	2.2 ± 0.1	16.5	10	1.28 ± 0.05	2.14 ± 0.03	
	50	1.10 ± 0.08	1.9 ± 0.1		50	1.65 ± 0.23	2.06 ± 0.02	
	90	1.06 ± 0.04	1.6 ± 0.1		90	2.05 ± 0.05	1.98 ± 0.03	
	130	1.05 ± 0.11	1.3 ± 0.1		130	2.55 ± 0.01	1.88 ± 0.03	
$\Delta H^{\ddagger}$, kJ/mol		77 ± 3	83 ± 4		41 ± 1	72 ± 2	72 ± 1	
$\Delta S^{\ddagger}$, J/mol·K		+94 ± 12	+61 ± 14		−45 ± 2	+12 ± 5	+10 ± 4	
$\Delta V^{\ddagger}$, cm^3/mol		+1.5 ± 0.3	+9.3 ± 0.5		−13.8 ± 0.4	+2.6 ± 0.2		

[a] Data obtained by NO-trapping method with the use of $[Ru^{III}(edta)(H_2O)]^-$, compare Figure S6 in Supporting Information.

respectively, is identical with that of $(P^{8+})Fe^{II}(NO)$, formed by the addition of NO to the reduced iron porphyrin, $(P^{8+})Fe^{II}$. The observed reaction pattern is outlined in eqs 4−5.

$$(P^{8+})Fe^{III}(H_2O)_2 + NO \underset{k_{off}}{\overset{k_{on}}{\rightleftharpoons}} (P^{8+})Fe^{II}(NO^+)(H_2O) + H_2O \quad (4)$$

$$(P^{8+})Fe^{II}(NO^+)(H_2O) \xrightarrow{+\,NO} (P^{8+})Fe^{II}(NO) + NO_2^- + 2\,H^+ \quad (5)$$

Because reaction 5 is considerably slower than 4 over the whole pH range studied, it did not interfere with the stopped-flow kinetic investigations on the reversible NO binding to $(P^{8+})Fe^{III}$. For clarity reasons, only kinetic data and mechanistic information for reaction 4 will be reported here. Studies on the subsequent reaction 5 for $(P^{8+})Fe^{III}$ (and other differently charged water-soluble iron(III) porphyrins) will be addressed in detail in a subsequent report.

Stopped-flow kinetic studies performed under pseudo-first-order conditions with NO in excess indicated that reaction 4 follows first-order kinetics, and the observed rate constants depend linearly on [NO], according to eq 6.

$$k_{obs} = k_{on}[NO] + k_{off} \quad (6)$$

Detailed kinetic measurements in the temperature range 5−25 °C allowed for the determination of k_{on} and k_{off} from the slopes and intercepts of the linear plots of k_{obs} versus [NO] at different temperatures (reported in Figure S2a, Supporting Information). Linear Eyring plots (see Figure S2b) allowed for the calculation of the activation parameters $\Delta H^{\ddagger}$ and $\Delta S^{\ddagger}$ for the "on" and "off" reactions. The corresponding activation volumes were obtained from stopped-flow kinetic measurements on the pressure dependence of k_{on} and k_{off} performed in the pressure range 10−130 MPa (see Supporting Information, Figure S3). The rate constants and activation parameters determined in these studies are summarized in Table 3.

Reversible Binding of NO to $(P^{8+})Fe^{III}(OH)(H_2O)$. Figure 5 reports the initial rapid spectral change resulting from mixing $(P^{8+})Fe^{III}(OH)(H_2O)$ and NO solutions at pH 8. The decrease in absorbance at 416 and 598 nm accompanied by an increase in absorbance at 434 and 548 nm features the formation of the nitrosyl product, $(P^{8+})Fe^{II}(NO^+)(OH)$. As also observed at pH 2, the NO binding step in basic solution is followed by the formation of $(P^{8+})Fe^{II}(NO)$ as the final reaction product. Due to insufficient stability of the initially formed $\{Fe-NO\}^6$ nitrosyl complex, characterization of its acid−base properties by spectrophotometric titration could not be performed. However, the difference in the positions of the Soret and Q-bands in its UV−vis spectrum (430 and 542 nm at pH 2, 434 and 548 nm at pH 8, respectively) is ascribed to the formation of a deprotonated form of the nitrosyl complex at high pH (viz. $(P^{8+})Fe^{II}(NO^+)(OH)$) on the basis of analogous shifts observed for $(P)Fe^{II}(NO^+)(L)$ species ($L = H_2O$, OH^-) formed by other water-soluble iron(III) porphyrins.[4] Hence, the NO binding to **1** at a high pH is described by reaction 7.

$$(P^{8+})Fe^{III}(OH)(H_2O) + NO \underset{k_{off}}{\overset{k_{on}}{\rightleftharpoons}} (P^{8+})Fe^{II}(NO^+)(OH) + H_2O \quad (7)$$

Kinetic studies on the reversible binding of NO to **1-OH** were performed at pH 8 according to similar experimental procedures as those employed for **1-H$_2$O**. Stopped-flow measurements at 25 °C allowed for the determination of the rate constants $k_{on} = 1.56 \times 10^3\ M^{-1}\ s^{-1}$ and $k_{off} = 6.22\ s^{-1}$ from the slope and intercept of the linear plot of k_{obs} versus [NO], respectively. Comparison with the corresponding values obtained at the same temperature at pH 2 (viz. $k_{on} = 15.1 \times 10^3\ M^{-1}\ s^{-1}$ and $k_{off} = 26.3\ s^{-1}$, see Table 3) shows that both the binding and release of NO are slower for **1-OH** as compared to those of **1-H$_2$O**. Systematic measurements of k_{on} and k_{off} values in buffered aqueous solutions in the pH range 2−8 resulted in the pH-rate profiles presented in Figure 6. The fit of the experimental data in Figure 6a and b to a sigmoidal function resulted in pK_a values of 5.11 ± 0.02 and 4.82 ± 0.02, respectively. The close similarity of both of these values to pK_{a1} of **1** indicate that the rate of NO binding and release is controlled by the nature of axial ligands in $(P^{8+})Fe^{III}(L)_2$ and decreases on going from **1-H$_2$O** to **1-OH**. A similar trend was observed previously for other water-soluble iron(III) porphyrins[4] (vide infra). Mechanistic

(27) Fernandez, B. O.; Lorkovic, I. M.; Ford, P. C. *Inorg. Chem.* **2004**, *43*, 5393 and references therein.

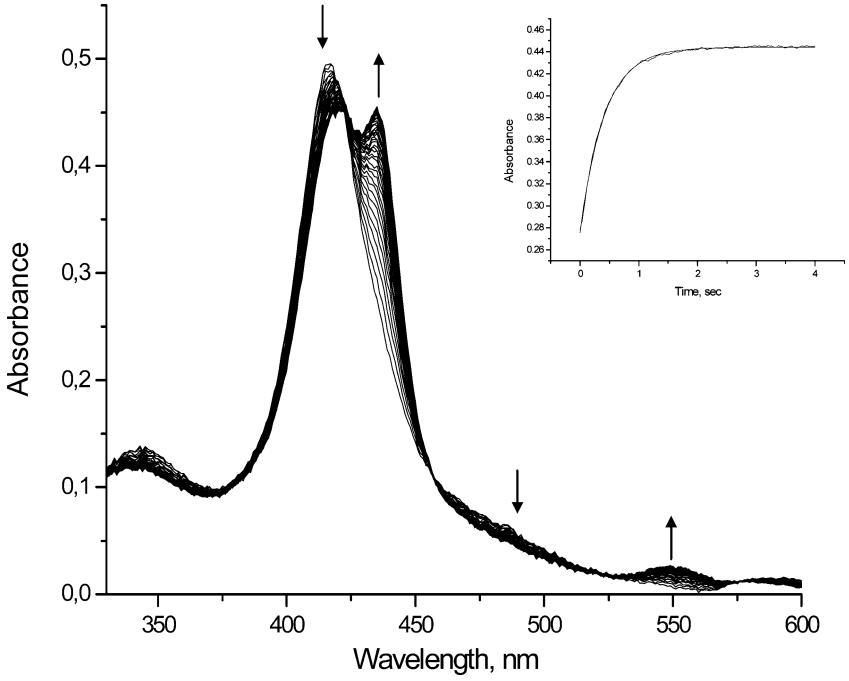

Figure 5. UV−vis spectral changes resulting from binding of NO (1×10^{-3} M) to **1-OH** (1×10^{-5} M) at pH 8 ($T = 10$ °C). (Inset) Fit of a kinetic trace recorded at 435 nm to a single-exponential function.

characterization of the reaction of **1-OH** with NO involved the measurement of k_{on} and k_{off} as a function of temperature and hydrostatic pressure, which provided $\Delta H^{\ddagger}$, $\Delta S^{\ddagger}$, and $\Delta V^{\ddagger}$ values for the binding and release of NO at a high pH. The experimental results obtained in these studies are summarized in Figures S4−S5 (Supporting Information) and in Table 3.

Mechanism of Reversible NO Binding to (P^{8+})Fe^{III}. Comparison with Other Water-Soluble Iron(III) Porphyrins.

A. Reactivity of (P^{8+})$Fe(H_2O)_2$ Toward NO. Mechanistic features of the reaction of **1-H_2O** with NO revealed that variable temperature and pressure studies can be best visualized by the volume profile constructed on the basis of $\Delta V^{\ddagger}_{on}$ and $\Delta V^{\ddagger}_{off}$ values, as presented in Figure 7. The positive sign of the activation volumes observed for both "on" and "off" reactions evidences a dissociatively activated mode of binding and release of NO from **1-H_2O**. As can be seen from the data summarized in Table 4, an analogous mechanistic picture was revealed by previously reported studies on NO binding to other (P)$Fe(H_2O)_2$. However, closer inspection of the data in Table 4 shows that the absolute values of $\Delta V^{\ddagger}_{on}$ and $\Delta V^{\ddagger}_{off}$, as well as the rate constants for the "on" and "off" reaction obtained for **1-H_2O**, are markedly smaller than the values reported for the other porphyrins. In fact, despite the limited number of complexes studied, clear reactivity trends can be identified for the (P)$Fe(H_2O)_2$ species reported in Table 4. These can be summarized as follows: (i) The rate of NO binding to (P)$Fe(H_2O)_2$ increases with increasing electron donation from the porphyrin meso substituents. The latter is reflected by increasing contribution of the intermediate $S = {}^3/_2$ spin state in the weakly spin admixed (P)$Fe(H_2O)_2$ complexes (int%).[4b,18,28] Hence, rela-

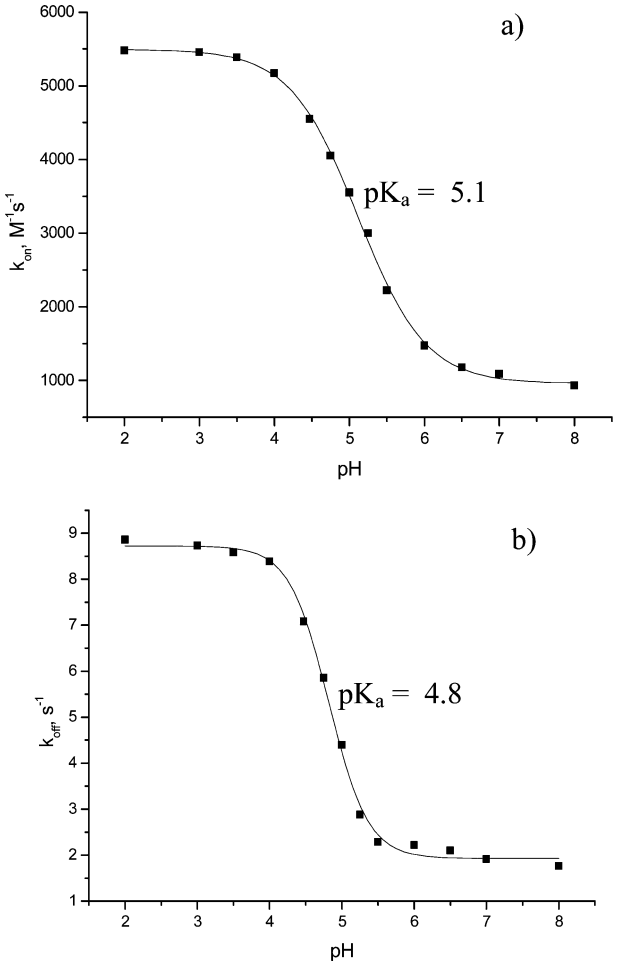

Figure 6. pH dependence of the rate constants k_{on} (a) and k_{off} (b) determined from the slopes and intercepts of linear plots of k_{obs} versus [NO], respectively, measured in the pH range 2.0−8.0. Experimental conditions [**1**] $= 2.5 \times 10^{-5}$ M, $T = 15$ °C, $I = 0.1$ M (adjusted with KNO_3); pH 2−3.5: chloroacetate buffer; pH 4−5.5: acetate buffer; pH 6−7: Bis-Tris; pH 8: Tris, [Buffer] = 0.05 M.

(28) Toney, G. E.; Gold, A.; Savrin, J.; Haar, L. W.; Sangaiah, R.; Hatfield, W. E. *Inorg. Chem.* **1984**, *23*, 4350.

Table 4. Rate Constants (at 298 K) and Activation Parameters for Reversible Binding of NO to a Series of Diaqua-Ligated Water-Soluble Iron(III) Porphyrins

				NO binding				NO release			
	iron(III) porphyrin	pK_{a1}	int%[a] (%)	$k_{on}/10^4$ $M^{-1}s^{-1}$	$\Delta H^{\ddagger}_{on}$ kJ/mol	$\Delta S^{\ddagger}_{on}$ J/mol·K	$\Delta V^{\ddagger}_{on}$ cm^3/mol	k_{off} s^{-1}	$\Delta H^{\ddagger}_{off}$ kJ/mol	$\Delta S^{\ddagger}_{off}$ J/mol·K	$\Delta V^{\ddagger}_{off}$ cm^3/mol
1	$(P^{8+})Fe$[b]	5.0	10	1.5 ± 0.1	77 ± 3	$+94 \pm 12$	$+1.5 \pm 0.3$	26.3 ± 0.5	83 ± 4	$+61 \pm 14$	$+9.3 \pm 0.5$
2	$(TMPyP^{4+})Fe$[c]	5.5	7	2.9 ± 0.2	67 ± 4	$+67 \pm 13$	$+3.9 \pm 1.0$	59 ± 4	108 ± 5	$+150 \pm 12$	$+16.6 \pm 0.2$
3	$(TPPS^{4-})Fe$[d]	7.0	20	50 ± 3	69 ± 3	$+95 \pm 10$	$+9 \pm 1$	500 ± 400	76 ± 6	$+60 \pm 11$	$+18 \pm 2$
4	$(P^{8-})Fe$[e]	9.3	24	82 ± 1	51 ± 1	$+40 \pm 2$	$+6.1 \pm 0.1$	220 ± 2	101 ± 2	$+140 \pm 7$	$+16.8 \pm 0.4$
5	$(TMPS^{4-})Fe$[d]	6.9	26	280 ± 20	57 ± 3	$+69 \pm 11$	$+13 \pm 1$	900 ± 200	84 ± 3	$+94 \pm 10$	$+17 \pm 3$

[a] Contribution of the intermediate spin state ($S = {}^3/_2$) in the spin-admixed $(P)Fe^{III}(H_2O)_2$ porphyrins, calculated on the basis of the empirical equation int% = $[(80 - \delta)/140] \times 100$, where δ is the chemical shift of the β-pyrrole ^1H, compare ref 18. [b] This work. [c] Reference 3a. [d] Reference 30. [e] Reference 4b

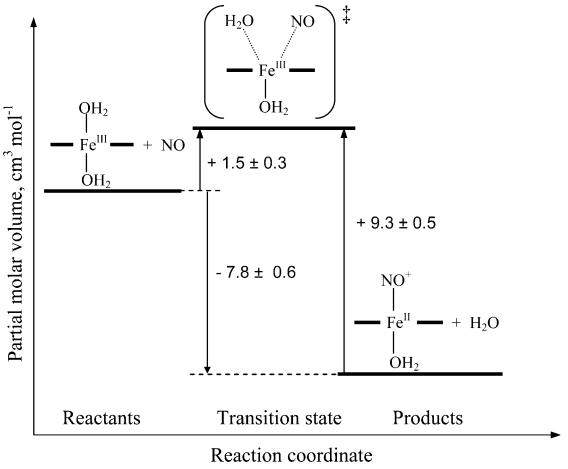

Figure 7. Volume profile for the reversible binding of nitric oxide to **1-H_2O**.

tively slow NO coordination rates observed for **1-H_2O** and **2-H_2O** with electron-withdrawing meso substituents become faster in $(P^{n-})Fe(H_2O)_2$ species **3**−**5**, for which increasing electron donation from the porphyrin ligand (reflected by the rising int%)[29] is observed. (ii) On the basis of the $\Delta V^{\ddagger}_{on}$ values determined for the diaqua species **1**−**5**, it may be concluded that the mechanism of the "on" reaction changes from predominantly dissociative in **5-H_2O** to interchange ($\mathbf{I}_d$ or **I**) in **1-H_2O**. Notably, the reactivity trends in (i) and (ii) are analogous to that observed for the water-exchange process on $(P)Fe(H_2O)_2$. This is in line with earlier conclusions[1a−b,5,30] that NO binding to diaqua-ligated iron(III) porphyrins is controlled by the rate-limiting water displacement step. It is evident from (i) and (ii) that a porphyrin-induced increase in electron density on the iron(III) center facilitates breakage of the Fe−OH_2 bond and induces a dissociative mechanism. Conversely, the presence of electron-withdrawing meso substituents in the porphyrin periphery stabilizes the Fe−H_2O bond to such an extent that an **I** mechanism (without a predominant **a**- or **d**-character) for NO coordination to the highly positively charged **1-H_2O** is energetically preferred over a dissociative pathway. (iii) An increase in k_{off} on going from $(P^{n+})Fe^{III}(H_2O)_2$ to $(P^{n-})Fe^{III}(H_2O)_2$ shows that the release of NO from $(P)Fe^{II}(NO^+)(H_2O)$ is facilitated by electron-donating meso substituents, whereas positively charged meso groups apparently stabilize the $Fe^{II}-NO^+$ bond, making the NO dissociation step relatively slow. This observation agrees with the recent computational and experimental results reported for a series of {FeNO}[6] porphyrin nitrosyls, which indicated that the addition of electron density at the meso carbon positions weakens the Fe−NO bond.[31] (iv) A substantially smaller $\Delta V^{\ddagger}_{off}$ observed for $(P^{8+})Fe^{II}(NO^+)(H_2O)$ (viz. $+9.3$ cm^3 mol^{-1}), as compared to the values reported for other porphyrin nitrosyls ($\Delta V^{\ddagger}_{off} \approx +17$ cm^3 mol^{-1}), implies a less dissociative mode for NO release in highly positively charged $(P^{8+})Fe^{II}(NO^+)(H_2O)$. In general, the large positive $\Delta V^{\ddagger}_{off}$ values found for NO dissociation from various porphyrin nitrosyls were interpreted in terms of a **d**-activated mechanism, in which the rate-limiting breakage of the $Fe^{II}-NO^+$ bond is accompanied by a significant volume increase due to the lengthening of the Fe−NO bond, spin change at the iron(III) center, and solvational changes.[1a−b,3a,30] Taking into account that NO coordination to **1-H_2O** follows an **I** mechanism, the principle of microscopic reversibility requires that the reverse process, i.e., breakage of the Fe−NO bond in $(P^{8+})Fe^{II}(NO^+)(H_2O)$, leads to the transition state in which the degree of bond formation with the entering water molecule is substantial. This is supposed to offset (to some extent) other positive contributions to the observed activation volume.

Taking into account the very different structural and electronic features of the meso substituents in **1**−**5**, it is likely that, in addition to their electronic influence, other (in particular steric and electrostatic) factors affect (to a varying extent) the kinetics and mechanism of NO binding and release in the individual porphyrin complexes. For example, a somewhat smaller k_{off} value observed for **4** as compared to those for **3** and **5** (where the electron-donating influence of the porphyrin ligand on the iron center is quite similar to that in **4**, as evidenced by similar int% values determined for **3**−**5**) may possibly result from the stabilization of a bound NO ligand in $(P^{8-})Fe^{II}(NO^+)(H_2O)$ via through-space electrostatic interactions with $-COO^-$ groups of the flexible malonato substituents. Furthermore, despite the slightly larger

(29) The inducing effect of porphyrin substituents is also reflected by the pK_a values of coordinated water in $(P)Fe(H_2O)_2$. However, due to the fact that the acidity of coordinated water may easily be influenced by other factors (in particular by through-space electrostatic interactions with charged groups in the porphiryn periphery), the int% value is used preferentially as a measure of the electronic influence of meso substituents in the porphyrin systems addressed in this work.

(30) Laverman, L. E.; Ford, P. C. *J. Am. Chem. Soc.* **2001**, *123*, 11614.

(31) (a) Linder, D. P.; Rodgers, K. R.; Banister, J.; Wyllie, G. R. A.; Ellison, M. K.; Scheidt, W. R. *J. Am. Chem.* Soc. **2004**, *126*, 14136. (b) Linder, D. P.; Rodgers, K. R. *J. Am. Chem. Soc.* **2005**, *44*, 1367.

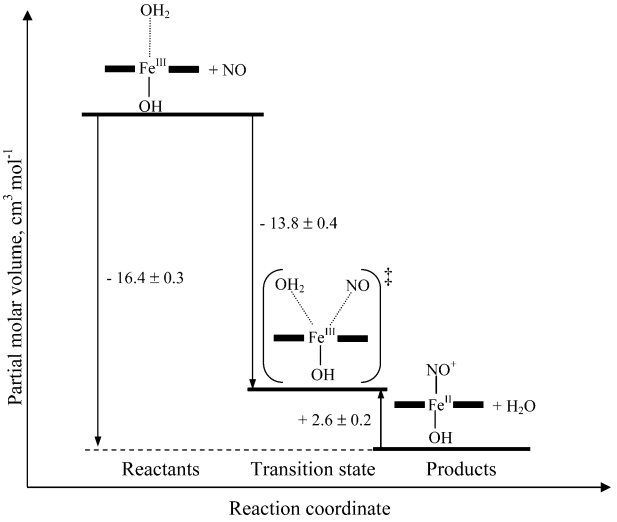

Figure 8. Volume profile for the reversible binding of nitric oxide to **1-OH**.

int% value calculated for **1** as compared to that of **2** (which suggests a longer Fe−H_2O bond and, consequently, a more labile iron center in **1**), the k_{ex} and k_{on} values measured for **1** are smaller than the corresponding values reported for **2**. This may reflect greater steric crowding around the iron center in **1**, where the presence of bulky meso substituents may impede formation of the transition state along an interchange mechanistic pathway assigned for **1**. This contrasts the situation in the open-faced porphyrin **2**, where access of the entering ligand to the metal center is very facile. Nevertheless, although the influence of steric and electrostatic effects should not be neglected in considering the reactivity of a given porphyrin system toward NO, the data in Table 4 suggest that modulation of electron density on the iron center by the porphyrin macrocycle is the main factor tuning the dynamics of reversible NO binding to (P)Fe^{III}(H_2O)$_2$.

B. Reactivity of (P^{8+})Fe(OH)(H_2O) Toward NO. As already stated in our earlier reports that addressed the reactivity of ferric porphyrins toward NO as a function of pH,[4] kinetic and mechanistic features of reversible NO binding to (P)Fe(OH) differ entirely from those observed for the diaqua-ligated forms. Although NO coordination to (P)Fe(H_2O)$_2$ is **d**-activated, an associative activation mode was observed for nitrosylation of (P)Fe(OH). It was also concluded that the rate of NO binding to (P)Fe(OH) is controlled by an Fe−NO bond-formation step rather than by the lability of the iron center. Due to electronic reasons (see below), the formation of the Fe−NO bond apparently exhibits a higher activation barrier in (P)Fe(OH) as compared to (P)Fe(H_2O)$_2$, such that a decrease in k_{on} (as well as in k_{off}) is observed at a high pH. These earlier conclusions are nicely illustrated by the experimental results obtained for (P^{8+})Fe(OH)(H_2O). The associative nature of NO coordination to **1-OH** is evident from the volume profile depicted in Figure 8. That the rate of NO coordination to **1-OH** is not controlled by the lability of the metal center is obvious from opposite effects of increasing pH on the values of k_{ex} and k_{on}; whereas a faster water-exchange rate at high pH indicates an increase in the lability of coordinated water in **1-OH** as compared to that in **1-H_2O**, the rate of NO binding decreases at a high pH. The latter effect is ascribed to electronic and structural changes, which determine the free energy barrier associated with the Fe−NO bond-formation step. These mainly involve the reorganization of spin density at the iron(III) center ($S = {}^3/_2$, ${}^5/_2 \rightarrow S = 0$ at low pH; $S = {}^5/_2 \rightarrow S = 0$ at high pH) along with structural changes accompanying this process. It was argued[4] that larger spin (and structural) changes accompanying the formation and breakage of the Fe^{II}−NO$^+$ bond in the purely high-spin monohydroxo-ligated species (as compared to those of the spin-admixed diaqua-ligated forms) lead to a higher activation barrier for NO coordination and release, thus decreasing the rate of these reactions at high pH.[4] The results obtained for **1** are in line with these earlier conclusions. In addition, although the number of monohydroxo-ligated porphyrin complexes studied with regard to their reaction with NO is admittedly limited, the data in Table 5 (which summarizes presently available kinetic and mechanistic information on these reactions) allow some additional comments to be made. It is evident from the data in Tables 4 and 5 that the rate of NO coordination and release is, in all studied cases, slower for monohydroxo-ligated porphyrins as compared to that for (P)Fe(H_2O)$_2$, and the NO binding is **a**-activated (in contrast to a **d**-activated mode observed at low pH). Furthermore, the k_{on} values measured for diaqua-ligated porphyrins vary within ca. 2 orders of magnitude and tend to correlate with the int% calculated for a given (P)Fe(H_2O)$_2$ complex, whereas differences in the NO binding rates are relatively small for various monohydroxo-ligated porphyrins. This again points to the different nature of the rate-limiting step for NO binding at low and high pH. Because the lability of the metal center is the decisive factor for the rate of NO binding at low pH, its increase (correlating with higher int%) results in a faster NO-binding rate. On the contrary, electronic and structural factors governing the rate-limiting Fe−NO bond formation at high pH are expected to vary relatively little for different (P)Fe(OH) species, which all represent purely high-spin porphyrin complexes.

It follows from the data summarized in Table 6 that the relative decrease in the values of k_{on} and k_{off} on going from a diaqua- to a monohydroxo-ligated (P)Fe^{III} complex varies considerably among the complexes studied. In particular, whereas for (TMPS)Fe^{III} (**5**) the rate constants for the "on" and "off" reactions decrease ca. 190 and 90-fold, respectively, at high pH, much smaller changes in k_{on} and k_{off} are observed for **1**. It can be argued that these differences reflect different electronic and structural features of **1** and **5**. Due to a relatively large contribution of the $S = {}^3/_2$ spin state in **5-H_2O**, considerable tetragonal distortion (manifested by short Fe−N_p and elongated axial bonds) is expected for this complex, in line with the observed lability of the iron center in **5-H_2O**. A comparison of typical structural features of six-coordinate spin-admixed porphyrins[26,32] with those of low-spin {FeNO}^{6} porphyrin nitrosyls[1c] (see Figure 9) also suggests that rather small structural changes occur upon the formation (and breakage) of the Fe−NO bond in spin-admixed **5-H_2O**. Thus, due to a facile substitution step and

Table 5. Rate Constants (at 298 K) and Activation Parameters for Reversible Binding of NO to Water-Soluble Monohydroxo-Ligated Iron(III) Porphyrins

			NO binding				NO release			
	iron(III) porphyrin	pK_{a1}	$k_{on}/10^4$ $M^{-1}\,s^{-1}$	$\Delta H^{\ddagger}_{on}$ kJ/mol	$\Delta S^{\ddagger}_{on}$ J/mol·K	$\Delta V^{\ddagger}_{on}$ cm^3/mol	k_{off} s^{-1}	$\Delta H^{\ddagger}_{off}$ kJ/mol	$\Delta S^{\ddagger}_{off}$ J/mol·K	$\Delta V^{\ddagger}_{off}$ cm^3/mol
1	$(P^{8+})Fe$[a]	5.0	0.16 ± 0.01	41 ± 1	-45 ± 2	-13.8 ± 0.4	6.2 ± 0.1	72 ± 2	$+12 \pm 5$	$+2.6 \pm 0.2$
2	$(TMPyP^{4+})Fe$ [b]	5.5	0.36 ± 0.01	41.4 ± 0.5	-38 ± 5	-13.7 ± 0.6	3.2 ± 0.1	78 ± 2	$+25 \pm 7$	$+9.5 \pm 0.8$
5	$(TMPS^{4-})Fe$[c]	6.9	1.46 ± 0.02 [d]	28.1 ± 0.6	-128 ± 2	-16.2 ± 0.4	10.5 ± 0.2 [d]	90 ± 1	$+77 \pm 3$	$+7.4 \pm 1.0$
4	$(P^{8-})Fe$ [e]	9.3	5.1 ± 0.2 [f]	34.6 ± 0.4	-39 ± 1	-6.1 ± 0.2	11.4 ± 0.3 [f]	107 ± 2	$+136 \pm 7$	$+17 \pm 3$

[a] This work. [b] Details of mechanistic studies performed within this work for **2**-OH are reported in Figures S7−8 and in Table S1 of Supporting Information. [c] Reference 4a. [d] Calculated for 298 K from the Eyring plots reported in ref 4a. [e] Reference 4b. [f] At 297 K.

Table 6. Ratio of Rate Constants Observed for the NO Binding ($k_{on}^{H_2O}/k_{on}^{OH}$) and NO Release ($k_{off}^{H_2O}/k_{off}^{OH}$) for Selected Water-Soluble Iron(III) Porphyrins

	iron porphyrin	int%	$k_{on}^{H_2O}/k_{on}^{OH}$	$k_{off}^{H_2O}/k_{off}^{OH}$
1	$(P^{8+})Fe$	10	9.4	4.2
2	$(TMPyP^{4+})Fe$	7	8.0	18.4
4	$(P^{8+})Fe$	24	16	19.3
5	$(TMPS^{4-})Fe$	26	192	85

relatively small electronic and structural changes, the energy barrier associated with reversible NO binding to **5-H_2O** is expected to be small. In contrast, the reaction of NO with purely high-spin five-coordinate **5-OH** involves greater reorganization of spin density at the metal center ($S = {}^5/_2 \rightarrow S = 0$, as compared to $S = {}^3/_2$, ${}^5/_2 \rightarrow S = 0$ at low pH) and larger structural changes (i.e., movement of the iron center into the porphyrin plane, a change in the coordination number, and contraction of the Fe−N_p bonds). As a consequence, large differences are observed in the kinetics of the reaction of **5** with NO at low and high pH, respectively. In the case of **1** the degree of spin admixture in diaqua-ligated **1-H_2O** is small, i.e., the complex is almost purely high spin. Furthermore, the excessive positive charge on the porphyrin stabilizes the axial Fe−H_2O bonds, making the NO coordination at low pH relatively slow. The high-spin **1-OH** complex formed at high pH is most probably six-coordinate, with the iron(III) center placed in the porphyrin plane.[26] Thus, in the case of **1**, electronic and structural changes upon the coordination (and release) of NO to **1-H_2O** and **1-OH**, respectively, are presumably quite similar, resulting in small differences in k_{on} and k_{off} values at low and high pH. However, because both k_{on} and k_{off} values may be influenced by various additional factors in (P)Fe^{III} complexes (such as steric crowding, through-space electrostatic interactions of axial ligands with charged porphyrin substituents, etc.), the scatter in the changes in k_{on} and k_{off} values for complexes reported in Table 6 is not surprising in view of their widely different steric, electronic, and structural features.

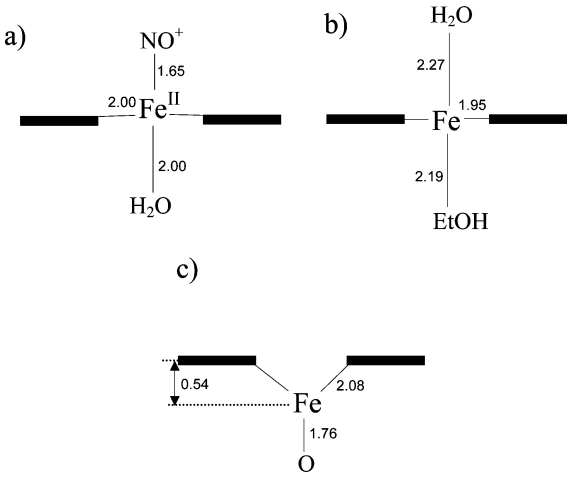

Figure 9. Typical structural features of Fe(III) porphyrins: (a) low-spin (TPP)$Fe^{II}(NO^+)(H_2O)$[1c], (b) admixed intermediate-spin (P)Fe(EtOH)(H_2O) complex (P = tetramethylchiroporphyrin) exhibiting large $S = {}^3/_2$ contribution in the ground spin state[32a], and (c) five-coordinate high-spin (P)Fe−O unit of the μ-oxo bridged dimer (TPP)Fe−O−Fe(TPP).[33]

Examination of the activation volumes for the "on" and "off" reactions of monohydroxo-ligated complexes reported in Table 5 allows two further comments. First, based on the differences in the $\Delta V^{\ddagger}_{on}$ and $\Delta V^{\ddagger}_{off}$ values among the complexes studied, it may be concluded that the transition state in the **a**-activated binding of NO occurs at different positions along the reaction coordinate. The activation volumes measured for the "on" and "off" reactions in **4-OH**, viz. $\Delta V^{\ddagger}_{on} = -6.1$ $cm^3\,mol^{-1}$ and $\Delta V^{\ddagger}_{off} = +17$ $cm^3\,mol^{-1}$, suggest an "early" transition state for this reaction, whereas the corresponding values for **1-OH** point to a "late" transition state. Second, the overall volume change calculated for **1** (viz. -16.4 $cm^3\,mol^{-1}$) is smaller than those observed for **2**−**4** (ca. -23 $cm^3\,mol^{-1}$). This difference can be ascribed to the presence of a weakly bound water molecule in **1-OH**, which is released from the complex upon coordination of NO, partially compensating the volume decrease associated with the formation of the $Fe^{II}-NO^+$ bond. Such a partial compensation is not expected for the five-coordinate (P)Fe(OH) species, which are (presumably) the predominant forms of **2**−**5** at pH > pK_{a1}.

Conclusions

The results of kinetic and mechanistic studies on the reversible binding of NO to **1** are in line with our earlier observations that the reactivity of model water-soluble iron(III) porphyrins toward nitric oxide is tuned by the pH of

(32) (a) Simonato, J.-P.; Pecaut, J.; Le Pape, L.; Oddou, J.-L.; Jeandey, C.; Shang, M.; Scheidt, W. R.; Wojaczyński, J.; Wołowiec, S.; Latos-Grażyński, L.; Marchon, J.-C. *Inorg. Chem.* **2000**, *39*, 3978. (b) Safo, M. K.; Schmidt, W. R.; Gupta, G. P.; Orosz, R. D.; Reed, Ch. A. *Inorg. Chim. Acta* **1991**, *184*, 251. (c) Cheng, B.; Scheidt, W. R. *Acta Crystallogr., Sect. C: Cryst. Struct. Commun.* **1995**, *57*, 1271. (d) Körber, F. C. F.; Lindsay Smith, J. R.; Prince, S.; Rizkallah, P.; Reynolds, C. D.; Shawcross, D. R. *J. Chem. Soc., Dalton Trans.* **1991**, 3291.

(33) (a) Hoffman, A. B.; Collins, D. M.; Day, V. W.; Fleischer, E. B.; Srivastava, R. S.; Hoard, J. L. *J. Am. Chem. Soc.* **1972**, *94*, 3620. (b) Swepston, P. N.; Ibers, J. A. *Acta Crystallogr., Sect. C: Cryst. Struct. Commun.* 1985, *41*, 671.

the solution.[4] In this context, the pH-induced change from diaqua- to monohydroxo-ligated porphyrin slows down the binding and release of NO and results in a mechanistic changeover in the coordination of NO to the iron(III) center. A comparison of experimental data obtained for **1** with those reported for other water-soluble $(P)Fe^{III}$ porphyrins clearly shows that the nature and charge of substituents in the porphyrin periphery affect the dynamics of both the binding and release of NO. These effects are particularly evident in the reactions of diaqua-ligated porphyrins, where the effective electron density on the metal center influences the lability of coordinated water (which determines the rate of the "on" reaction) and the strength of the Fe−NO bond in the $\{FeNO\}^6$ product (as evidenced by variation in k_{off} values determined for the complexes studied). Other (mainly steric and electrostatic) factors are likely to influence the binding and/or release of NO in specific porphyrin systems. Despite a rather limited set of studied porphyrins, it can be concluded on the basis of the available data that reversible binding of NO to iron(III) porphyrins is very sensitive to the nature of axial ligands and the porphyrin periphery. The NO^+ ligand in the $\{FeNO\}^6$ nitrosyl formed by **1** undergoes subsequent reductive nitrosylation to form $(P^{8+})Fe^{II}NO$ ($\{FeNO\}^7$ nitrosyl) as the final reaction product. This reaction will be addressed in detail along with data for related complexes in a following report.

The important role of electronic, structural, and environmental factors (especially pH) on the reactivity of the studied porphyrin complexes toward NO can be of biological significance. Although the pH ranges selected to differentiate between the reactivity pattern of the diaqua and hydroxo complexes are in some cases far away from biological conditions, local effects in the catalytic "pockets" of enzymes can induce a drastic change in the apparent acidity and result in a mechanistic changeover, as reported in this study.

Acknowledgment. We gratefully acknowledge financial support from the Deutsche Forschungsgemeinschaft within SFB 583 "Redox-active metal complexes".

Supporting Information Available: Figures S1−8 and Table S1. This material is available free of charge via the Internet at http://pubs.acs.org.

IC051339V